23rd ABCM International Congress of Mechanical Engineering
December 6-11, 2015, Rio de Janeiro, RJ, Brazil

ELASTO-VISCOPLASTIC BEHAVIOR OF A POLYVINYLIDENE FLUORIDE (PVDF) IN TENSION

João Marciano Laredo dos Reis
jreis@mec.uff.br
Heraldo Silva da Costa Mattos
heraldo@mec.uff.br
Eduardo Pereira Motta
edupmotta@msn.com

Theoretical and Applied Mechanics Laboratory – LMTA, Mechanical Engineering Post Graduate Program – PGMEC, Universidade Federal Fluminense – UFF, Rua Passo da Pátria, 156 Bl. E sala 216, Niterói, RJ, Brazil

Abstract. *The present paper is concerned with the plasticity of a polyvinylidene fluoride (PVDF) in tension. Strain rate strongly influences the plastic behavior, but the variation of the elastic properties is almost negligible within the range of strain rates considered in the study (from 1.6 x 10-4 s-1 up to 1.6 x 10-1 s-1). In particular, the yield stress and the ultimate tensile strength are strongly rate-dependent. A one-dimensional elasto-viscoplastic phenomenological model is proposed and analyzed. Despite the nonlinearity of the model equations, only one tensile test performed with variable strain rate is sufficient to identify all material parameters. Model predictions are compared with experiments showing good agreement.*

Keywords: *PVDF; Tensile tests; Tensile tests; Strain rate; Constitutive modeling; Elasto-viscoplasticity;*

1. INTRODUCTION

Offshore oil drilling and exploration in increasingly deep waters requires the replacement of traditional structures and metallic materials for others with less linear weight and higher strength.

The polymeric layers work as sealing, insulating and/or anti-wear components, whilst the metallic layers withstand the imposed structural loads. Since the mid-1980s, there has been an increasing growth in the use of flexible pipes in ultra-deep offshore oil exploration [6]. Knowledge of mechanical properties of polymers used as pressure sheaths of offshore flexible pipes is crucial for guaranteeing safe operation.

Therefore, the present paper will study the elasto-viscoplasticity of a pressure sheath made of PVDF, which is a semicrystalline engineering polymer that exhibits high mechanical toughness as well as remarkable functional properties [2].

Many investigations have been carried out to characterize the chemical structure of PVDF [5], but only a few studies are concerned with its macroscopic mechanical behavior. Technical information about the mechanical behavior is required for any polymer used in offshore applications. In particular, the present study is concerned with the mechanical behavior of a PVDF sample taken from a riser pressure sheath in tension.

Tensile tests at ambient temperature have been performed under variable load rates (from 1.6 x 10-4 s-1 up to 1.6 x 10-1 s-1). One of the main features of PVDF is elasto-viscoplasticity: the plastic behavior is strongly rate dependent while the elastic properties are almost rate-insensitive.

The main goal of this paper is to propose a one-dimensional phenomenological model for describing the behavior of PVDF in tensile tests varying strain rates at ambient temperature. The model equations combine enough mathematical simplicity to allow their application to engineering problems with the capability of describing complex nonlinear mechanical behaviour (irreversible deformations and strain rate sensitivity observed in tensile tests performed at different strain rates). The material constants that appear in the model can be easily identified from just one stress-strain curve obtained at different strain rates.The model equations can be obtained within the thermodynamic context described in previous works by da Costa Mattos et al. [1-5].

2. MATERIALS AND METHODS

2.1 MATERIALS

PVDF is a highly non-reactive and pure thermoplastic fluoropolymer produced by the polymerization of vinylidene difluoride. This kind of polymer is increasingly finding use as a material for pressure sheaths of flexible pipes where operating conditions are particularly severe. Tensile specimens of a particular polyvinylidene fluoride were machined from the internal sheath of a real flexible pipe. The initial gage length l_0 and initial cross section A_0 of the specimen were, respectively, 33 mm and 24 mm^2, as illustrated in Fig. 1.

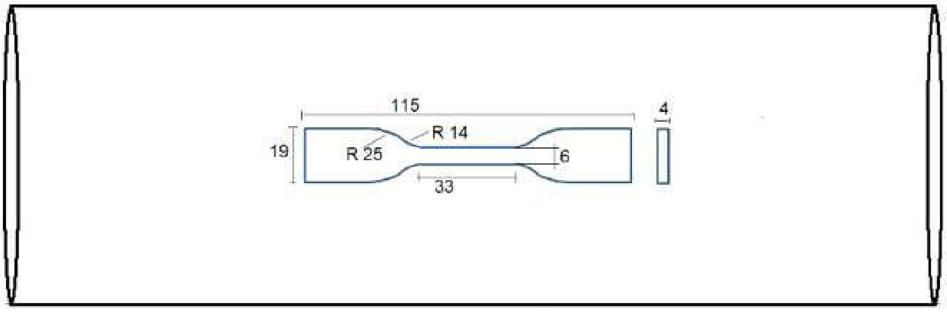

Figure 1. Tensile test specimen

2.2 METHODS

Mechanical tensile tests at different strain rates were performed using a Shimadzu® AG-X universal testing machine and electro-mechanical sensors for the control of longitudinal strain in the active zone of the test specimens. Tensile tests at four different prescribed engineering strain rates, 1.6 x 10-4s-1, 1.6 x 10-3s-1, 1.6 x 10-2s-1 and 1.6 x 10- 1s-1 were performed to quantify the strain rate dependency of PVDF. The strain rates were chosen based on ASTM D 638-08 [7] and the previous work performed by the authors [5]. Also, a tensile test with varying strain rate was performed in order to evaluate the strain rate dependency of PVDF.

3. RESULTS AND DISCUSSION

3.1 EXPERIMENTS

The classical uniaxial engineering stress and engineering strain will be denoted, respectively, σ and ε:

$$\sigma = \frac{F(t)}{A_0} \quad ; \quad \varepsilon(t) = \frac{\Delta l(t)}{l_0} \tag{1}$$

F(t) is the axial force necessary to impose an elongation Δl(t) at a given instant t. l_0 is the gauge length and A_0 the cross-section area. Assuming constant volume, the true stress and true strain can be defined as:

$$\sigma_t = \sigma(1+\varepsilon) \quad ; \quad \varepsilon_t = ln\,(1+\epsilon) \tag{2}$$

Figure 2 presents the true stress vs. true strain curves for PVDF obtained from the controlled-strain tensile tests at different constant engineering strain rates, $\dot{\varepsilon}_1 = 1.6 \text{ x } 10^{-4}\text{s}^{-1}$, $\dot{\varepsilon}_2 = 1.6 \text{ x } 10^{-3}\text{s}^{-1}$, $\dot{\varepsilon}_3 = 1.6 \text{ x } 10^{-2}\text{s}^{-1}$ and $\dot{\varepsilon}_4 = 1.6 \text{ x } 10^{-1}\text{s}^{-1}$.

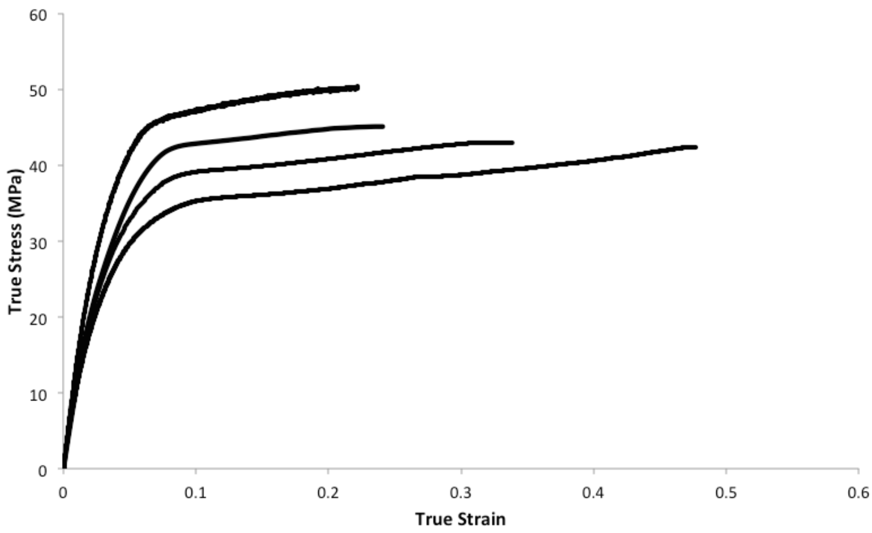

Figure 2. True stress vs. true strain curves of PVDF at different strain rates

The curves display a significant strain rate dependency in which the maximum strength and yield stress increase as the strain rate increases. The elastic modulus remains almost constant. The deformation is very uniform without the presence of necking before rupture.

To analyze the elasto-viscoplastic behavior, it is interesting to split the true strain into two parts: an elastic part ε^e and a plastic part ε^p, defined as follows:

$$\varepsilon_t = \varepsilon^e + \varepsilon^p \text{ with } \varepsilon^e = \frac{\sigma_t}{E} \text{ and } \varepsilon^p = \varepsilon_t - \frac{\sigma_t}{E} \tag{3}$$

Since $E = 1.12\ GPa$ is a constant, effects of strain rate dependency are only observed in the plastic part ε^p. Thus, the main physical information is obtained through the true stress vs. true plastic strain curves.

The true stress vs. true plastic strain curves for PVDF at different constant engineering strain rates, $\dot{\varepsilon}_1 = 1.6 \text{ x } 10^{-4}\text{s}^{-1}$, $\dot{\varepsilon}_2 = 1.6 \text{ x } 10^{-3}\text{s}^{-1}$, $\dot{\varepsilon}_3 = 1.6 \text{ x } 10^{-2}\text{s}^{-1}$ and $\dot{\varepsilon}_4 = 1.6 \text{ x } 10^{-1}\text{s}^{-1}$ are presented in Fig. 3. It is possible to identify two different regions: (I) the first one, region I, where $(d\sigma^2/d\varepsilon^{p^2} < 0)$ and (II) a second one, region II, where $(d\sigma^2/d\varepsilon^{p^2} = 0)$. The transition plastic strain ε^p between regions I and II is almost a constant.

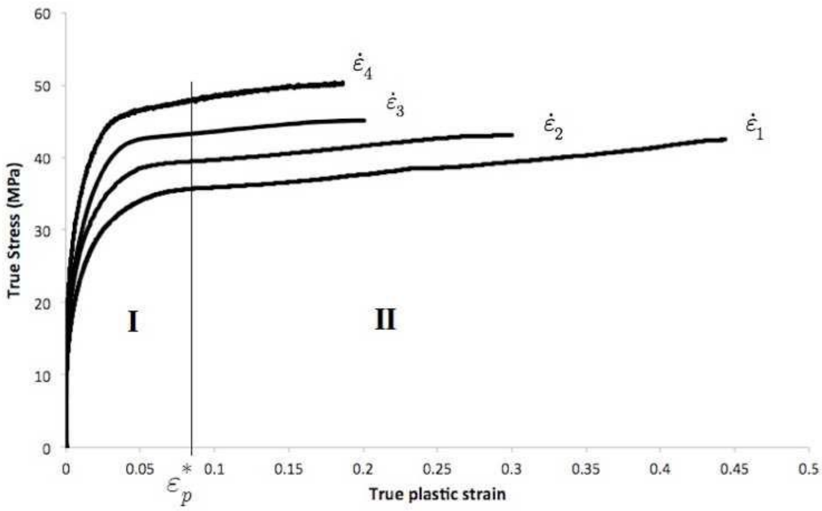

Figure 3. True stress vs. true plastic strain curves of PVDF at different strain rates

Fig. 4 presents the true stress vs. true plastic strain curves for PVDF with the strain rate varying in steps ($\dot{\varepsilon}_1 = 1.6 \text{ x } 10^{-4}\text{s}^{-1}$, $\dot{\varepsilon}_2 = 1.6 \text{ x } 10^{-3}\text{s}^{-1}$ and $\dot{\varepsilon}_3 = 1.6 \text{ x } 10^{-2}\text{s}^{-1}$). This curve is superposed on the previous ones and the curves coincide at each step. The small difference in the transition is due to the control system of the universal machine and to the inertia effects (the model assumes a quasi-static process with negligible inertia of the testing system).

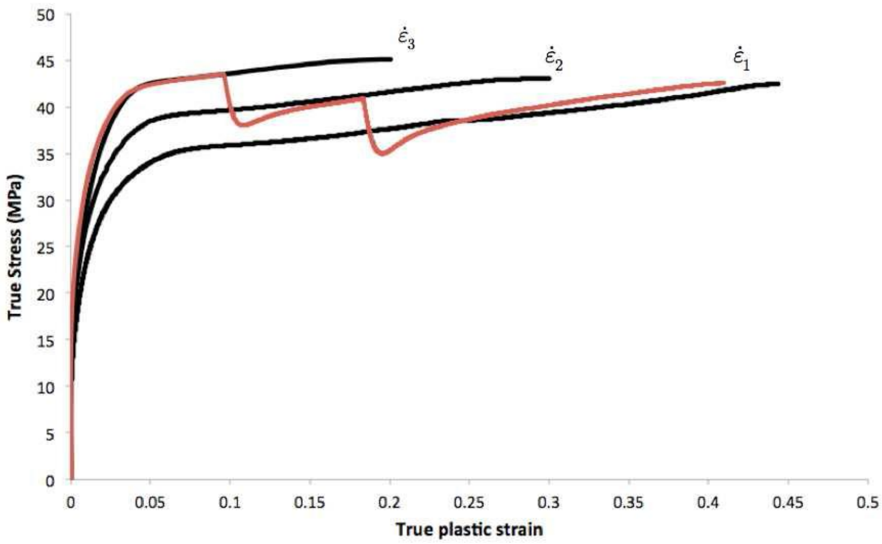

Figure 4 - true stress vs. true plastic strain curves for PVDF with the strain rate variation and with a single constant strain rate.

3.2 MODELING

The proposed phenomenological model for PVDF is divided into two parts, corresponding to the two regions observed in the experiments. The following relation between σ_t and ε^p is proposed:

$$\sigma_t = \sigma_0 + a(\varepsilon_t, \dot{\varepsilon}_t)\left[1 - \exp\left(-b(\varepsilon_t, \dot{\varepsilon}_t)\varepsilon_p\right)\right] + c\langle\varepsilon_t - \varepsilon_p^*\rangle \quad (4)$$

For $\sigma_t \geq \sigma_0$, with

$$a(\varepsilon_t, \dot{\varepsilon}_t) = a_1[\exp(\varepsilon_t)\dot{\varepsilon}_t]^{a_2} \quad (5)$$

$$b(\varepsilon_t, \dot{\varepsilon}_t) = b_1[\exp(\varepsilon_t)\dot{\varepsilon}_t]^{b_2} \quad (6)$$

Where $\langle\varepsilon_t - \varepsilon_p^*\rangle = \max\{\varepsilon_t - \varepsilon_p^*, 0\}$. σ_0, a_1, a_2, b_1, b_2 and c are positive material constants. Since the goal is to discuss the strain rate dependency, the model is restricted to monotonic loading histories within a given range of strain rates $\dot{\varepsilon}_{min} \leq \dot{\varepsilon} \leq \dot{\varepsilon}_{max}$. It is difficult to present a precise definition of the limiting strain rates $\dot{\varepsilon}_{min}$ and $\dot{\varepsilon}_{max}$. In the absence of a precise physical definition, it is suggested that a range between $1.6 \times 10^{-4}\mathrm{s}^{-1}$ and $1.6 \times 10^{-1}\mathrm{s}^{-1}$.

3.3 IDENTIFICATION OF THE PARAMETERS ($\boldsymbol{a_1}$, $\boldsymbol{a_2}$, $\boldsymbol{b_1}$, $\boldsymbol{b_2}$)

The parameters σ_0, ε_p^* and c can be easily identified. $\sigma_0 = 15$ MPa is the yield stress, above which irreversible deformation appears ($\sigma_t = \sigma_0$ if $\varepsilon_p = 0$). As mentioned in the previous section, the proposed model is divided into two parts, and in the present case $\varepsilon_p^* \approx 0.08$. The parameter c is the slope of the second part of the true stress vs plastic strain curve.

The following procedure can be used to identify the material constants (a_1, a_2, b_1, b_2) that appear in Eqs. (4-6). From definition (2), it is possible to relate the rate of the engineering strain $\dot{\varepsilon}$ with the rate of real strain $\dot{\varepsilon}_t$ as follows:

$$\varepsilon_t = \ln(1+\varepsilon) \Rightarrow \exp(\varepsilon_t) = \exp(ln(1+\varepsilon)) \Rightarrow \varepsilon = \exp(\varepsilon_t) - 1 \Rightarrow \dot{\varepsilon} = \exp(\varepsilon_t)\,\dot{\varepsilon}_t \Rightarrow \dot{\varepsilon}_t = \frac{\dot{\varepsilon}}{(1+\varepsilon)} \quad (7)$$

Hence, the equation that models the initial part of the test (eq. 4), at constant engineering strain rate, can be expressed as:

$$\sigma_t = \sigma_0 + a(\dot{\varepsilon})[1 - \exp(-b(\dot{\varepsilon})\varepsilon_p)] \quad (8)$$

Thus, from equation (8), it is also possible to conclude that:

$$\lim_{\varepsilon_p = \varepsilon_p^{\cdot}}(\sigma_t - \sigma_0) \approx \lim_{\varepsilon_p = \infty}(\sigma_t - \sigma_0) = a(\dot{\varepsilon}) \quad (9)$$

From equation (8), it follows that $\sigma_t = \sigma_0 + a(\dot{\varepsilon})$ is the maximum value of the stress σ_t for a given constant strain rate, as shown in Fig. 6. It can also be verified that:

$$\left.\frac{d(\sigma_t - \sigma_0)}{d\varepsilon_p}\right|_{\varepsilon_p = 0} = a(\dot{\varepsilon})b(\dot{\varepsilon}) \quad (10)$$

If $a(\dot{\varepsilon})$ is known, $b(\dot{\varepsilon})$ can be identified from the slope of the true stress vs. true plastic strain curve, as shown in Fig. 5. The parameters a_1, a_2, b_1, b_2 can be identified from the experimental curves log(a)x log($\dot{\varepsilon}$) and log(b)x log($\dot{\varepsilon}$). They can be obtained from only two different tests at constant engineering strain rates since the behavior of these curves is linear. Therefore:

$$a = a_1(\dot{\varepsilon})^{a_2} \Rightarrow \log(a_1) + a_2\log(\dot{\varepsilon}) \quad (11)$$

$$b = b_1(\dot{\varepsilon})^{b_2} \Rightarrow \log(b_1) + b_2\log(\dot{\varepsilon}) \quad (12)$$

Taking two arbitrary strain rates $\dot{\varepsilon}_1$ and $\dot{\varepsilon}_2$ (it is suggested that the maximum and minimum admissible rates for the model are: $1.6 \times 10^{-4}\mathrm{s}^{-1}$ and $1.6 \times 10^{-1}\mathrm{s}^{-1}$) and using the experimental values $a(\dot{\varepsilon}_1)$, $a(\dot{\varepsilon}_2)$, it is possible to identify the parameters a_2 and b_2:

$$a(\dot{\varepsilon}_1) = \log(a_1) + a_2 \log(\dot{\varepsilon}_1)\,;\; a(\dot{\varepsilon}_2) = \log(a_1) + a_2 \log(\dot{\varepsilon}_2) \tag{13}$$

$$b(\dot{\varepsilon}_1) = \log(a_1) + b_2 \log(\dot{\varepsilon}_1)\,;\; b(\dot{\varepsilon}_2) = \log(b_1) + b_2 \log(\dot{\varepsilon}_2) \tag{14}$$

Combining the equations in (13) and (14) it is possible to obtain:

$$a_2 = \frac{[\log(\dot{\varepsilon}_1) - \log(\dot{\varepsilon}_2)]}{[a(\dot{\varepsilon}_1) - a(\dot{\varepsilon}_2)]}\,;\; b_2 = \frac{[\log(\dot{\varepsilon}_1) - \log(\dot{\varepsilon}_2)]}{[b(\dot{\varepsilon}_1) - b(\dot{\varepsilon}_2)]} \tag{15}$$

Once a_2 and b_2 are determined, it is possible to obtain a_1 and b_1 using the equations (13) and (14). Figure 5 shows the identification of the $a(\dot{\varepsilon})$ and $b(\dot{\varepsilon})$ parameters from the true stress vs. true plastic strain curve:

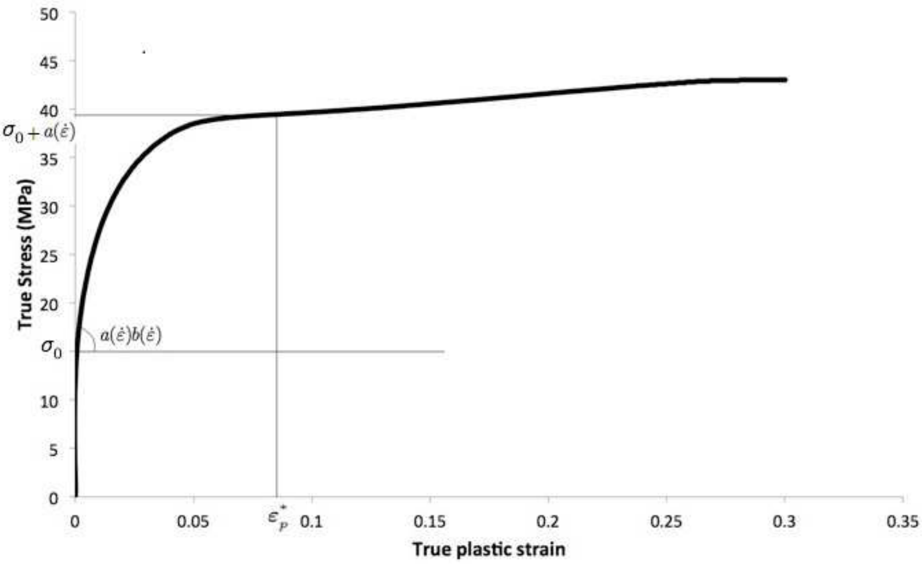

Figure 5. Identification of $a(\dot{\varepsilon})$ and $b(\dot{\varepsilon})$ parameters from the true stress vs. true plastic strain curve

An alternative procedure that requires only one tensile test (with variable strain rate Fig. 6) to obtain the constants a_1, a_2, b_1, b_2 can be considered.

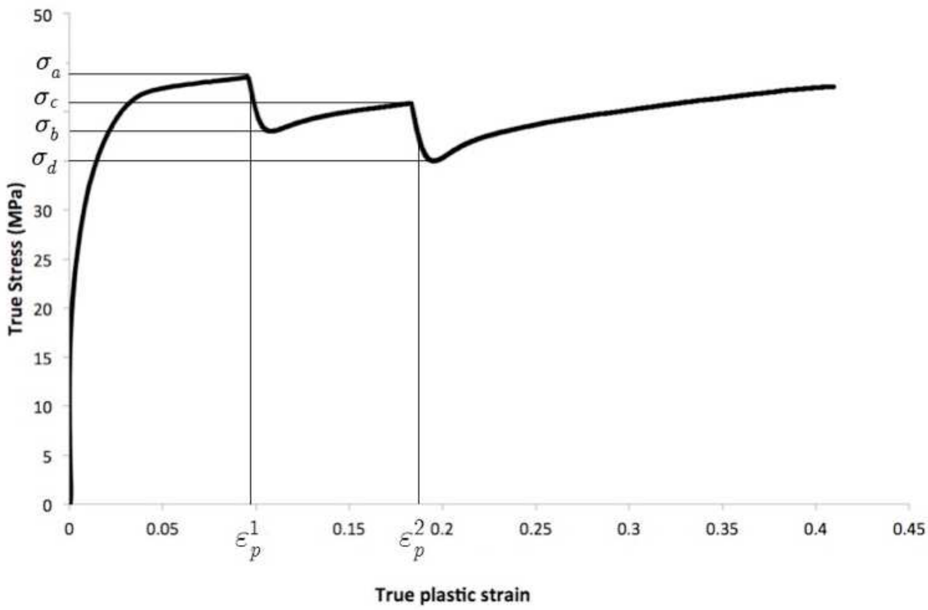

Figure 6. Strain rate variation context in the tensile true stress vs. true strain of PVDF.

In Fig. 6, the test starts with $\dot{\varepsilon}_3 = 1.6 \times 10^{-2}\mathrm{s}^{-1}$, then, the strain rate is changed to $= 1.6 \times 10^{-3}\mathrm{s}^{-1}$ and, finally, changed to $\dot{\varepsilon}_1 = 1.6 \times 10^{-4}\mathrm{s}^{-1}$. ε_p^1 and ε_p^2 are the plastic strain where there is a change in the strain rate. The following set of nonlinear algebraic equations are obtained:

$$\begin{aligned}
\sigma_a &= \sigma_0 + a_1(\dot{\varepsilon}_3)^{a_2}\left[1 - \exp\left(-b_1(\dot{\varepsilon}_3)^{b_2}\dot{\varepsilon}_3\varepsilon_p^1\right)\right] + c\langle\varepsilon_p^1 - \varepsilon_p^*\rangle \\
\sigma_b &= \sigma_0 + a_1(\dot{\varepsilon}_2)^{a_2}\left[1 - \exp\left(-b_1(\dot{\varepsilon}_2)^{b_2}\dot{\varepsilon}_2\varepsilon_p^1\right)\right] + c\langle\varepsilon_p^1 - \varepsilon_p^*\rangle \\
\sigma_c &= \sigma_0 + a_1(\dot{\varepsilon}_2)^{a_2}\left[1 - \exp\left(-b_1(\dot{\varepsilon}_2)^{b_2}\dot{\varepsilon}_2\varepsilon_p^2\right)\right] + c\langle\varepsilon_p^2 - \varepsilon_p^*\rangle \\
\sigma_d &= \sigma_0 + a_1(\dot{\varepsilon}_2)^{a_2}\left[1 - \exp\left(-b_1(\dot{\varepsilon}_1)^{b_2}\dot{\varepsilon}_1\varepsilon_p^2\right)\right] + c\langle\varepsilon_p^2 - \varepsilon_p^*\rangle
\end{aligned} \tag{16}$$

The constants a_1, a_2, b_1, $b_2$can be identified using (16) and a least squares technique. The values of (a_1, a_2, b_1, b_2) obtained using the two procedures are almost identical, and are presented in table 1, together with the other material constants.

Table 1. Material parameters.

a_1(MPa)	a_2	b_1	b_2	σ_0(MPa)	ε_p^*	c (MPa)	E (GPa)
35.85	6.13×10^{-2}	114.44	9.26×10^{-2}	15	8.00×10^{-2}	18	1.12

3.4 COMPARISON BETWEEN MODEL PREDICTION AND EXPERIMENTAL RESULTS

To determine the accuracy of the model, all tests have been compared with the model predictions. Fig. 7 presents the experimental and theoretical true stress vs. true plastic strain curves for different strain rates.

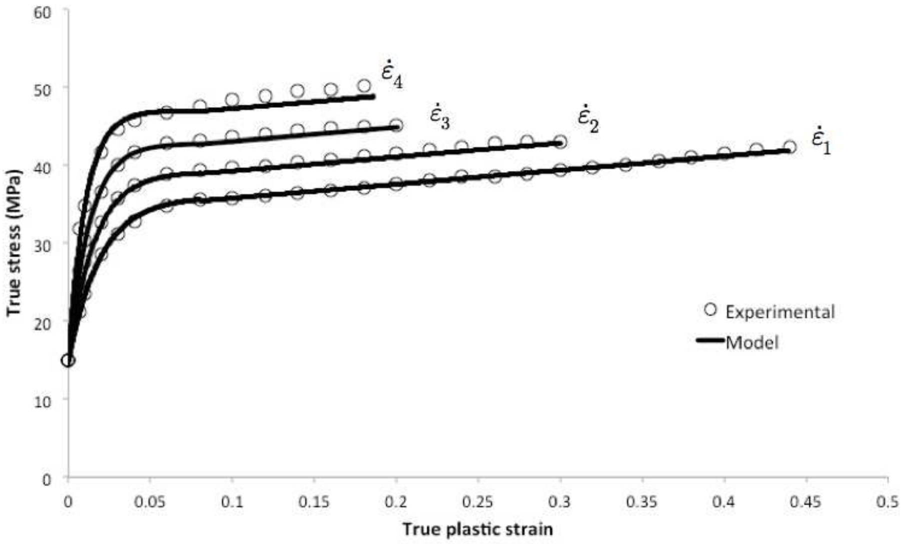

Figure 7. PVDF experimental and theoretical true stress vs. true plastic strain curves for different strain rates.

It can be verified that, despite the strong nonlinear behavior of the material, the experimental results are in good agreement with the model predictions. It is important to emphasize that, although test results for four different strain rates are presented, only one test was used to identify the material parameters (Fig. 6).

Fig. 8 presents the experimental and theoretical true stress vs. true plastic strain curves for the variable strain rate.

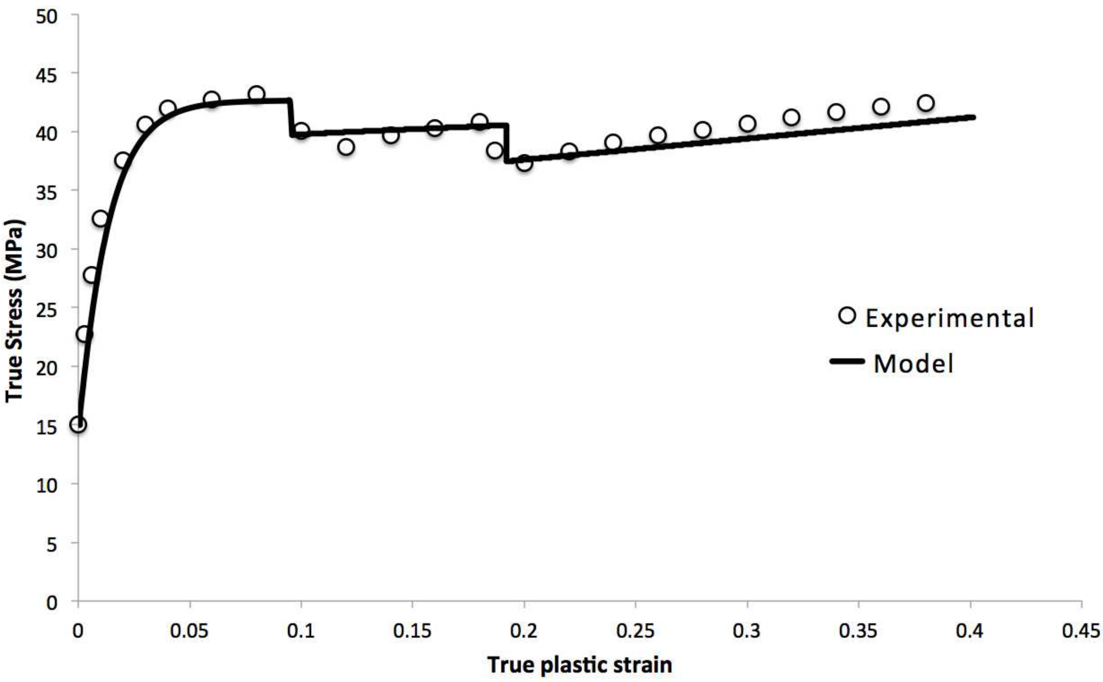

Figure 8. True stress vs. true plastic strain curves. Comparison between model predictions and experiments.

It can be seen from Fig. 8 that the model predicts well the experimental results for variable loading rates with small discrepancies due to the inertia effects observed in the testing machine (it is impossible to impose an instantaneous change of velocity).

4. CONCLUSION

In this study, the strain rate dependency of a polyvinylidene fluoride (PVDF) used as internal pressure sheath material in flexible pipes is analyzed. The strain rate significantly influences the mechanical behavior of PVDF in tensile tests. An elastoviscoplastic model, able to describe such a dependency, was also proposed. This model combines simplicity to allow its usage in practical problems with a physically realistic description of the mechanical behavior of PVDF in monotonic tensile tests with variable strain rate. The goal is to use this model to obtain the maximum amount of information about the macroscopic properties of PVDF from a minimum number of laboratory tests, saving time and experimental costs. The experimental identification of the material parameters that arise in the theory is simple, requiring one tensile test with variable engineering strain rate or two tensile tests with constant engineering strain rate. The model predictions have good correlation with experimental results obtained in tensile tests performed using constant and variable strain rates.

5. ACKNOWLEDGEMENTS

The authors thank the Research Foundation of the State of Rio de Janeiro (FAPERJ), the Brazilian National Council for Scientific and Technological Development (CNPq) and Coordination for the Improvement of Higher Education Personnel (CAPES) for supporting part of the work presented here.

6. REFERENCES

[1] da Costa Mattos HS, Bastos IN, Gomes JACP. A simple model for slow strain rate and constant load corrosion tests of austenitic stainless steel in acid aqueous solution containing sodium chloride, Corros. Sci. 2008:50;2858.

[2] Do hany JE. Poly(vinylidene fluoride). Encyclopedia of Chemical Technology, vol. 11, Wiley, New York. 1994.

[3] E l Mohajir B, Heymans N. Changes in structural and mechanical behavior of PVDF with processing and thermomechanical treatments. 1. Change in structure. Polymer 2001:42;5661.

[4] Nunes LCS, Dias FWR, da Costa Mattos HS. Mechanical behavior of polytetrafluoroethylene in tensile loading under different strain rates. Polym Test 2011:30:791.

[5] Reis JML, Pacheco LJ, da Costa Mattos HS. Tensile behavior of post-consumer recycled high-density polyethylene at different strain rates. Polym Test 2013:32:338.

[6] Saunder C. Extending design life, improving integrity of flexible pipe. 11 Jan. 2007. http://www. offshore-mag.com, accessed 28/01/2015. .

[7] S tandard Test Method for Tensile Properties of Plastics. ASTM ± D 638Ȝ08 .

7. RESPONSIBILITY NOTICE

The authors are the only responsible for the printed material included in this paper.